

ANL/CHM/CP-85318
CONF-950793--52

Diamond Films Grown from Fullerene Precursors*

Dieter M. Gruen, Christopher D. Zuiker, and Alan R. Krauss

Materials Science and Chemistry Divisions
Argonne National Laboratory
Argonne, Illinois 60439

RECEIVED
JAN 24 1995
OSTI

Submitted for the

Proceedings of the Fullerenes and Photonics II Conference,
Part of SPIE's 1995 International Symposium on
Optical Science, Engineering and Instrumentation
San Diego, California, July 9-14, 1995

July 1995

DISCLAIMER

This report was prepared as an account of work sponsored by an agency of the United States Government. Neither the United States Government nor any agency thereof, nor any of their employees, makes any warranty, express or implied, or assumes any legal liability or responsibility for the accuracy, completeness, or usefulness of any information, apparatus, product, or process disclosed, or represents that its use would not infringe privately owned rights. Reference herein to any specific commercial product, process, or service by trade name, trademark, manufacturer, or otherwise does not necessarily constitute or imply its endorsement, recommendation, or favoring by the United States Government or any agency thereof. The views and opinions of authors expressed herein do not necessarily state or reflect those of the United States Government or any agency thereof.

The submitted manuscript has been authored by a contractor of the U. S. Government under contract No. W-31-109-ENG-38. Accordingly, the U. S. Government retains a nonexclusive, royalty-free license to publish or reproduce the published form of this contribution, or allow others to do so, for U. S. Government purposes.

*Work supported by the U.S. Department of Energy, BES-Materials Sciences, under Contract W-31-109-ENG-38.

DISTRIBUTION OF THIS DOCUMENT IS UNLIMITED

MASTER

DISCLAIMER

**Portions of this document may be illegible
in electronic image products. Images are
produced from the best available original
document.**

Diamond films grown from fullerene precursors

Dieter M. Gruen, Christopher D. Zuiker, and Alan R. Krauss

Materials Science and Chemistry Divisions
Argonne National Laboratory, Argonne, Illinois 60439

ABSTRACT

Fullerene precursors have been shown to result in the growth of diamond films from argon microwave plasmas. In contradistinction to most diamond films grown using conventional methane-hydrogen mixtures, the fullerene-generated films are nanocrystalline and smooth on the nanometer scale. They have recently been shown to have friction coefficients approaching the values of natural diamond. It is clearly important to understand the development of surface morphology during film growth from fullerene precursors and to elucidate the factors leading to surface roughness when hydrogen is present in the chemical vapor deposition (CVD) gas mixtures. To achieve these goals, we are measuring surface reflectivity of diamond films growing on silicon substrates over a wide range of plasma processing conditions. A model for the interpretation of the laser interferometric data has been developed, which allows one to determine film growth rate, rms surface roughness, and bulk losses due to scattering and absorption. The rms roughness values determined by reflectivity are in good agreement with atomic force microscope (AFM) measurements. A number of techniques, including high-resolution transmission electron microscopy (HRTEM) and near-edge x-ray absorption fine structure (NEXAFS) measurements, have been used to characterize the films. A mechanism for diamond-film growth involving the C₂ molecule as a growth species will be presented. The mechanism is based on (1) the observation that the optical emission spectra of the fullerene-containing plasmas are dominated by the Swan bands of C₂ and (2) the ability of C₂ to insert directly into C-H and C-C bonds with low activation barriers, as shown by recent theoretical calculations of reactions of C₂ with carbon clusters.

Keywords: Fullerene precursors, diamond films, nanocrystalline, surface roughness, tribology, carbon dimer.

1. INTRODUCTION

The discovery of the fullerenes in 1985 was followed in 1990 by the prescription for preparing bulk amounts of these startling new allotropes of carbon.^{1,2} Buckminsterfullerene, C₆₀, the most plentiful of the new allotropes, has many unique chemical and physical properties that have attracted the attention of researchers around the world. Several of these properties are of particular interest from the point of view of the present work. C₆₀ is thermodynamically unstable with respect to graphite (9 kcal/g mol C) and to diamond (8.5 kcal/g mol C);³ contains no hydrogen; displays primarily intramolecular bonding, with attendant high volatility; and exhibits an unusual fragmentation pattern.

2. VOLATILITY AND PHOTOFRAGMENTATION OF C₆₀

The vapor pressure of C₆₀ is shown in Fig. 1. It can be seen that at 600 °C, the vapor pressure is 10⁻² Torr, which is equivalent to 0.6 Torr in terms of an elemental C vapor pressure.⁴ The vapor pressure of graphite reaches that value only if heated to ~ 3500 °C. It is astounding to realize that one now has available pure carbon vapor at quite modest temperatures.

Since 1985, photofragmentation of C₆₀ by intense laser irradiation has been known to display the pattern shown in Fig. 2. The mass peaks are separated by 24 mass units down to C₃₀ or C₂₈. The

interpretation given to this observation has generally been that fragmentation occurs by elimination of carbon dimers, C_2 , with subsequent cage reclosure.⁵ Presumably once the special stability of C_{60} has

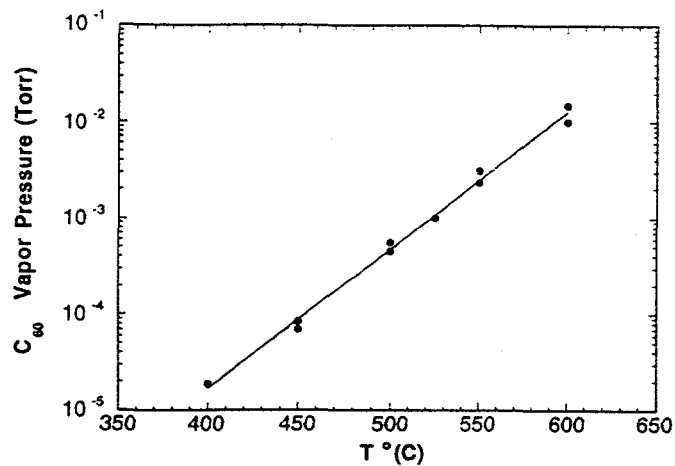


Fig. 1. Vapor pressure of C_{60} versus temperature T ($^{\circ}$ C).

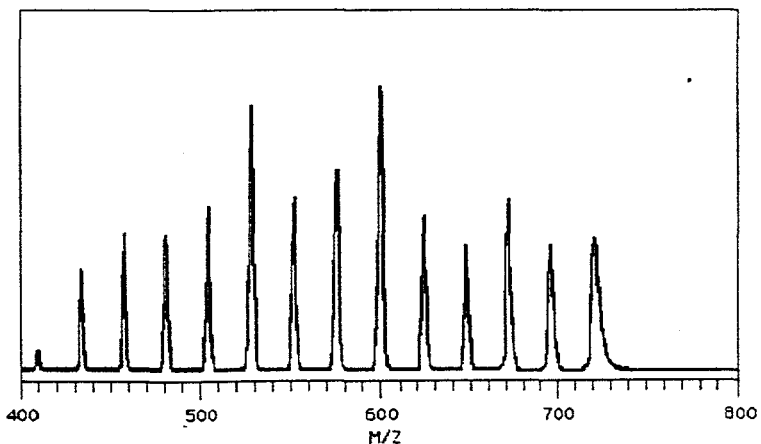


Fig. 2. Photofragmentation mass spectrum of C_{60} .

been breached, the smaller clusters are metastable and continue fragmenting in this way until the strain energy overwhelms the resonance energy, whereupon the cage opens. Fragmentation then proceeds to yield both even and odd, rather than only even, carbon clusters. The signature for cage opening is a mass gap between $\sim C_{28}$ and $\sim C_{12}$. The lower mass carbon cluster distribution is not shown in Fig. 2. The fragmentation pattern that has just been described is also observed when accelerated C_{60}^+ collides with surfaces⁶ or with stationary gases.⁷ The fragmentation of C_{60} has aroused considerable experimental⁸ as well as theoretical⁹ interest, but it is beyond the scope of the present paper to delve into this subject. Suffice it to say that fragmentation of C_{60} via C_2 elimination is highly unusual, since the vaporization thermodynamics of graphite are dominated by the odd carbon species, C , C_3 , C_5 , etc.¹⁰ Presumably in the case of C_{60} , the favorable free energy change for the reaction $C_{60} \rightarrow C_{58} + C_2$ is due to the additional energy gained when the cage recloses to eliminate dangling bonds.

Even though C_2 had never actually been seen in the mass spectra of fragmenting C_{60} , presumably because of its high (~ 12 ev) ionization potential, the evidence is quite strong that C_2 is indeed a plentiful primary product of C_{60} fragmentation. It should therefore be relatively straightforward to use C_{60} as a source of this highly reactive chemical species. In particular, we were fascinated by the intriguing possibility of using C_2 as a new species for growing diamond film.

3. HYDROCARBON VERSUS CARBON DIMER, C_2 , PRECURSORS

The extraordinary properties of diamond, its hardness, coefficient of friction, tensile strength, electrical resistivity, thermal conductivity, thermal shock resistance, and optical transmission, to name some of its outstanding characteristics, make diamond a material with many potential uses and future applications. The discovery and development of methods for the chemical vapor deposition of diamond film about twenty years ago has given a major impetus to finding ways of realizing the uses to which the properties of diamond lend themselves. Essentially all of the methods currently employed for diamond film CVD typically involve mixtures of 1-5% CH_4 or another hydrocarbon with 99-95% H_2 . In order for diamond film growth to occur, the molecular hydrogen must be dissociated to form atomic hydrogen. Atomic hydrogen is thought to be crucial to the diamond growth process using hydrocarbon precursors, because one needs to:¹¹

- (1) Create carbon radicals on the diamond surface;
- (2) Produce gas-phase methyl radicals (which adsorb on the carbon radicals);
- (3) Sustain sequential hydrogen abstraction reactions from the adsorbed methyl radicals;
- (4) Stabilize the diamond structure;
- (5) React with and remove graphitic nuclei.

The roles of atomic hydrogen in the growth of diamond films from hydrocarbon precursors outlined above have been extensively discussed.¹² Detailed mechanisms have been elaborated,¹³ which involve atomic hydrogen in many of the steps that ultimately lead to the incorporation of carbon from the hydrocarbon precursor into the diamond lattice.

It has recently been shown theoretically that in contradistinction to $CH_3\bullet$, C_2 can insert directly and with a low activation energy into the C-H bond.¹⁴ Therefore with C_2 as a growth species, requirement (1) above is obviated. With C_2 , hydrogen abstraction reactions are clearly superfluous, and requirements (2) and (3) are also obviated. The role of atomic hydrogen in satisfying requirements (4) and (5) is not clearly defined. With C_2 as a growth species, the presence of atomic hydrogen during the growth process would appear to be strongly relaxed and may perhaps not be necessary at all. The consequences of such a development could be far-reaching and could have important implications, both for the mechanism of diamond film growth and for the properties of the resulting films.

4. C_{60} FRAGMENTATION IN A MICROWAVE PLASMA

The approach we use to fragment C_{60} is to set up a microwave discharge in a C_{60}/Ar mixture using a commercially available (ASTEX PDS 17) plasma-enhanced chemical vapor deposition (PECVD) apparatus, as is shown schematically in Fig. 3. The only change from using the apparatus with conventional CH_4/H_2 mixtures is to attach a sidearm carrying a quartz tube surrounded by a tube furnace. An Ar-carrier gas is saturated with C_{60} by flowing the Ar over heated fullerene-containing soot at 500-600 °C. Film deposition is carried out with a gas flow of 100 sccm at a pressure of 80 Torr, a

microwave power of 1000 W, and a substrate temperature of 750-850 °C. Substrates used up to now have been Si, SiC, Si_3N_4 , W, WC, and Ni.

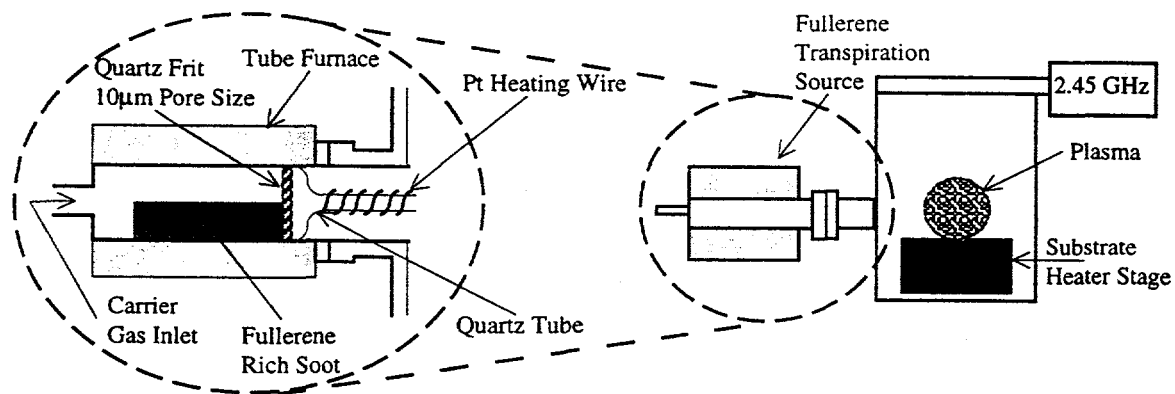


Fig. 3. Schematic diagram of microwave apparatus for the deposition of diamond film using C_{60} as a precursor molecule.

The plasma discharge is bright emerald green in color, and the emission measured by bringing the radiation to a spectrometer with a fiberoptic cable is dominated by the well-known Swan bands (Fig. 4) of C_2 , from which, by vibration analysis, one can deduce the vibrational temperature of C_2 .¹⁵

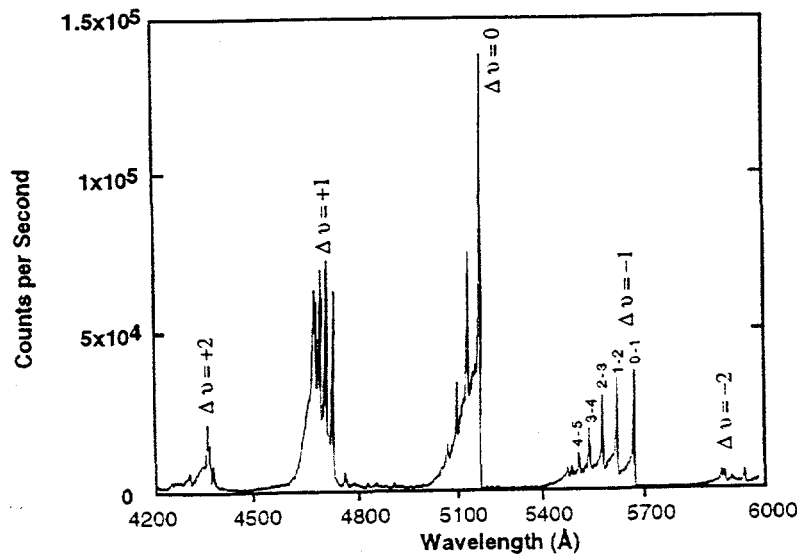


Fig. 4. Emission spectrum of C_{60}/Ar microwave discharge showing Swan Bands of C_2 .

To our knowledge, this is the first direct evidence that C_2 is in fact a principal product of C_{60} fragmentation. The plasma processes, by means of which the fragmentations of C_{60} are brought about, must include some or all of the following:

- (1) Absorption of microwave power by C_{60} ;
- (2) Collisionally induced dissociation (CID) by Ar;
- (3) Energy transfer from Ar^* ;
- (4) Charge exchange ($Ar^+ + C_{60} \rightarrow Ar + C_{60}^+$);
- (5) Photoprocesses;
- (6) Thermal decomposition of C_{60} ;
- (7) Electron impact processes.

It will require detailed study to assess the relative importance of these processes. It is likely that collisionally induced dissociation (CID) is the principal mechanism, but then, of course, one cannot clearly separate this process from energy transfer or charge exchange processes. We have begun an inquiry into these questions by setting up a time-of-flight mass spectrometer with which to sample the carbon cluster species produced in the plasma as a function of plasma parameters, such as microwave power and gas pressure.

5. IN SITU LASER INTERFEROMETRY OF DIAMOND FILM GROWTH

In order to monitor the film growth in situ, a HeNe laser interferometer is used, as is shown schematically in Fig. 5. By measuring the surface reflectivity of the substrate with time, the film thickness, growth rate, rms surface roughness, and bulk attenuation coefficient can be determined. To obtain these quantities from interference measurements, a model based on scalar scattering theory was developed.¹⁶ The model assumes random growth of the surface; the surface roughness $\delta \ll \lambda$, the laser wavelength; $\lambda \ll S$, the surface correlation length; $\delta \ll d$, the film thickness, which implies that the

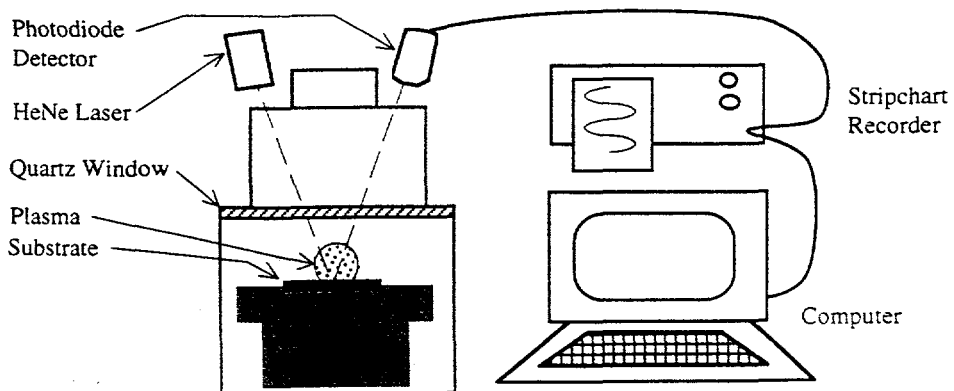


Fig. 5. Schematic diagram of laser interferometric measurements of diamond film growth characteristics.

diamond nuclei have coalesced and formed a coherent film; and the diamond-substrate interface is perfectly smooth, which is very close to the actual situation for a silicon substrate.

Bulk attenuation leads to a decrease in the reflectivity oscillation amplitude, while surface roughness leads to a decrease in both the oscillation amplitude as well as the average reflectivity. The surface roughness is of particular interest to our work with C₆₀ precursors, because we have found that films produced in this way are exceedingly smooth, with rms roughness in the 30-60 nm range (Fig. 6).

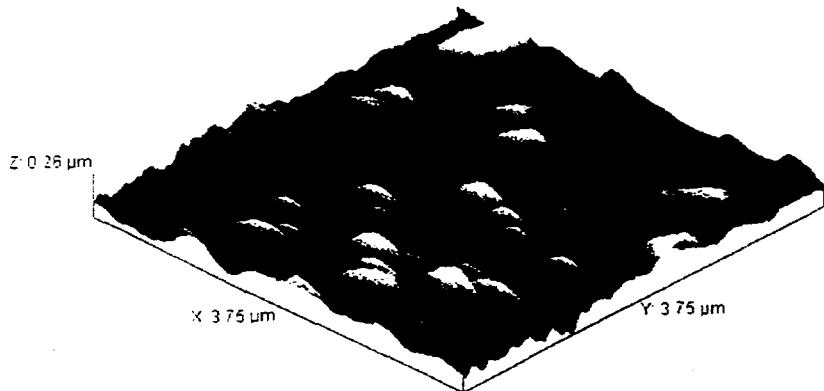


Fig. 6. Atomic force microscope image of a diamond film grown from a C₆₀/Ar microwave discharge.

In contradistinction, nonoriented diamond films grown from CH₄/H₂ mixtures have rms roughnesses, which are typically on the micron scale (Fig. 7).

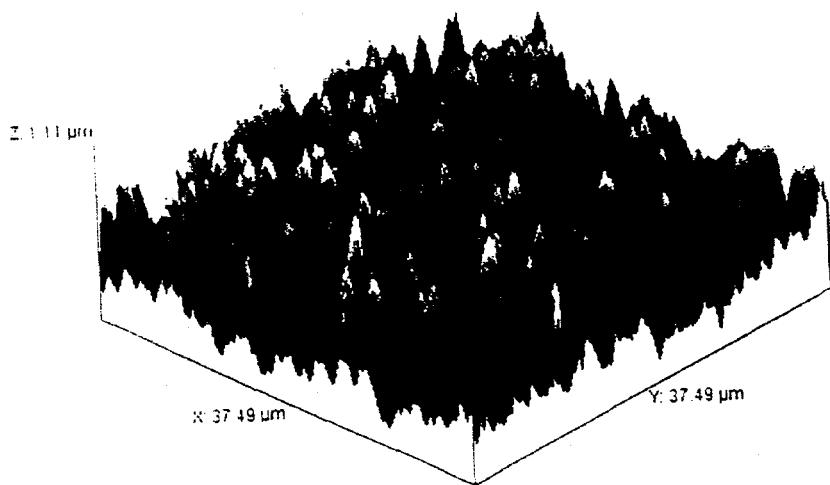


Fig. 7. Atomic force microscope image of a diamond film grown from a CH₄/H₂ microwave discharge.

For the surface roughness range of interest to the C₆₀ generated films, the 632.8 nm wavelength of the HeNe laser is the correct choice. The surface roughness, δ , is given by the expression

$$\delta = \frac{\lambda}{2\pi} \sqrt{\frac{1}{2} \ln \frac{2r_i}{\sqrt{R_{\max}} + \sqrt{R_{\min}}}} ,$$

where r_i is the reflectivity at the gas diamond interface, and R_{\max} and R_{\min} are the measured interference maxima and minima. The interferometrically determined δ 's are plotted against atomic force microscope measurements in Fig. 8. The agreement between the two measurements can be considered quite satisfactory. We therefore have a reliable way of monitoring *in situ* the surface roughness of the growing films and following that property as a function of changing plasma parameters.

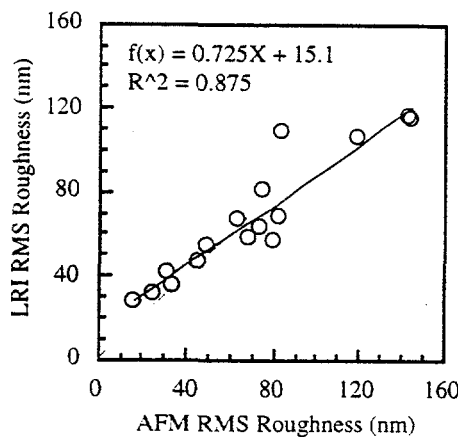


Fig. 8. Comparison of surface roughness measurements obtained by laser interferometry and by atomic force microscopy.

6. SURFACE MORPHOLOGY, MICROSTRUCTURE, AND TRIBOLOGY
 with J. Luo, R. Csentsis, and A. Erdemir, and C. Bindal
 Chemical Technology, Materials Science, and Energy Technology Divisions
 Argonne National Laboratory, Argonne, IL 60439

One must now inquire into the reasons for the difference in surface morphology seen in the C_{60} versus the hydrocarbon precursor films. It has been known for a long time that there is a connection between surface roughness and microstructure:¹⁷ the smaller the grain size, the smoother the surface. Transmission electron microscope (TEM) plan-view studies of C_{60} -generated films have shown that the deposits are nanocrystalline in nature,¹⁸ and that the nanocrystallites display very few structural defects. A high-resolution lattice image of a typical grain of dimension $\sim 10 \times 50$ nm is shown in Fig. 9. Grain sizes have been systematically measured on ~ 500 grains each in several different films, and the results are reproducible from one deposit to another. Grain size distributions peak at 13-15 nm, thus providing a rationale for the observed low values of surface roughness. Cross-section TEM images reveal several equiaxed diamond grains and continuous nucleation of new grains throughout the thickness of the film.

The nanocrystalline microstructure of the films is totally consistent with the nanometer scale surface roughness, which in turn should translate into low friction coefficients.¹⁹ The friction coefficient of Si_3N_4 and SiC pins sliding against these smooth surfaces have been measured and are in the range 0.05-0.10, comparable to the values observed with natural diamond. The friction coefficients are lower by factors of 5 to 10, compared with rough diamond films grown by conventional CH_4/H_2 methodologies. The wear rate on a Si_3N_4 pin sliding against a C_{60} -derived film in air at ambient temperature for 2.4×10^6 cycles (35 km) with a 5-Newton load was $1.4 \times 10^{-8} \text{ mm}^3/\text{N}\cdot\text{m}$, one-to-two orders of magnitude lower than normally observed on diamond films. A profilometric trace of the film

after the sliding experiment described above is shown in Fig. 10. One observes a wear track ~ 1 μm in depth, demonstrating the low level of abrasion and ploughing produced as a result of the tribological test.



Fig. 9. Transmission electron microscopy (TEM) plan-view lattice image of a typical diamond nanocrystallite deposited from a C_60/Ar microwave discharge.

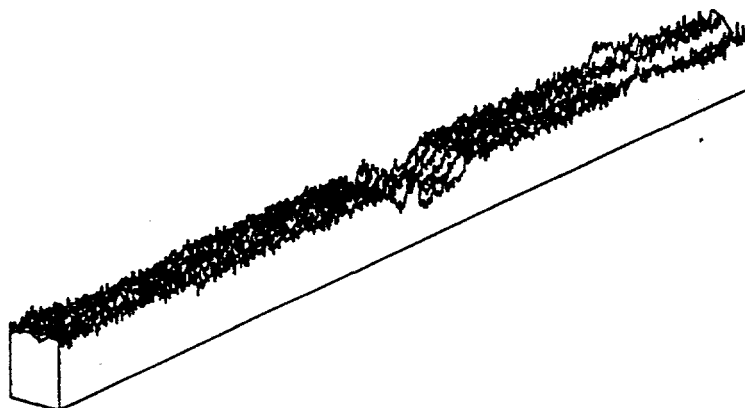


Fig. 10. Profilometric trace of a C_60/Ar -generated diamond film subsequent to tribological testing with a Si_3N_4 pin. (5N load; 2.4×10^6 cycles; wear rate = $1.4 \times 10^{-8}\text{mm}^3/\text{N}\cdot\text{m}$).

7. CHARACTERIZATION OF DIAMOND FILMS

with L. Terminello and J. Carlisle
Chemistry and Materials Science Directorate
Lawrence Livermore National Laboratory, Livermore, CA 94550

In general, growth of diamond films by CVD involves a competitive process of nucleation and growth among various forms of carbon: diamond, graphite, or amorphous carbon. Bachmann et al.²⁰ reported, based on gas compositions and experimentally grown diamond films over the past twenty years, that the formation domain for the diamond phase is compositionally quite narrowly defined within a triangular portion of a C-H-O diagram. As has already been pointed out, it is generally believed that a large excess of hydrogen is indispensable for the nucleation and growth of the diamond phase. It is therefore necessary to show that pure diamond is grown under the conditions described in the present work, where the hydrogen content is at most 1-2% of the total gas mixture and the oxygen content is even lower.

A variety of techniques has been used to characterize the C₆₀-derived films. X-ray diffraction (XRD) shows <111> to be the most prominent reflection, followed by <220> and <311>. Lines due to graphite are never seen. Electron diffraction rings taken on the nanocrystals in TEM are indexed solely on the diamond lattice. Electron energy loss spectra (EELS) taken in conjunction with the TEM measurements show only a σ loss feature, and there is no evidence of a π loss feature. Raman spectroscopy shows in addition to the 1331 cm⁻¹ feature due to the well-known diamond phonon band, a broad band with a maximum at 1550 cm⁻¹, usually attributed to nondiamond carbon. The interpretation of this band has been and still is the subject of considerable discussion in the literature. On the basis of our measured grain-size distribution, we calculate that about 3% of the carbon in the films is surface carbon situated at grain boundaries. Such surface carbon can find itself in various bonding situations, such as π -bonding, or terminated by hydrogen. It is not unreasonable to expect that Raman scattering by surface carbon is more pronounced than by bulk carbon, and that even a few percent of surface carbon could account for the broad band at 1550 cm⁻¹ seen in our Raman spectra.

The relatively recent development of C1s NEXAFS measurements using synchrotron radiation has opened a new and significant chapter in the area of diamond film characterization. Results from such measurements on graphite and diamond reference materials are shown in Fig. 11, together with results on a C₆₀/Ar-derived film, a 1% CH₄-99% H₂ film, a laser-ablated carbon film, and an amorphous diamondlike carbon (DLC) film. The C1s photoabsorption spectra of diamond and graphite show a very

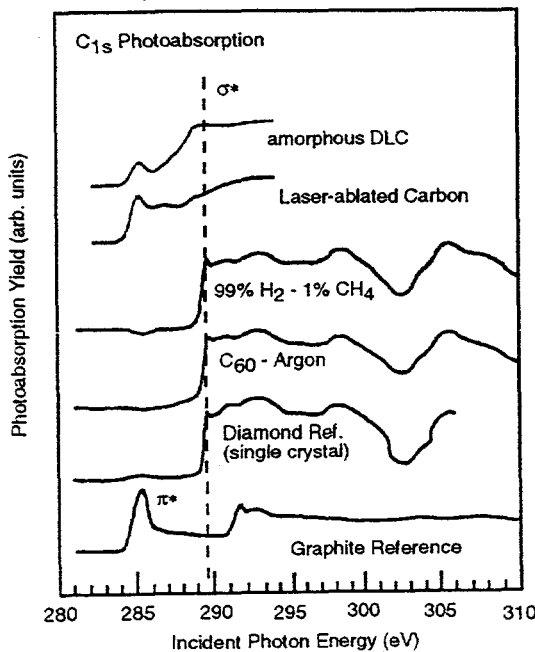


Fig. 11. NEXAFS photoabsorption spectra of the C1s edge of graphite, diamond, and various carbon films.

clear distinction between the σ^* and π^* absorption features, indicating that this is a powerful new methodology for distinguishing between these two forms of carbon. Amorphous carbon is found to be much more similar to graphite than to diamond in its C1s signature. Both the C₆₀-derived and the CH₄-derived films are indistinguishable one from the other and in turn indistinguishable from the diamond reference spectrum. We conclude that our C₆₀/Ar-derived films are in fact pure or nearly pure diamond, since there is no evidence of any graphitic or amorphous phase. This conclusion is in accord with all of the data from TEM, electron diffraction, and XRD measurements on C₆₀-derived films that we have obtained in the course of our studies.

8. MECHANISM OF DIAMOND FILM GROWTH WITH C₂ AS A GROWTH SPECIES
with L. Curtiss, D. Horner, and P. Redfern
Chemical Technology Division
Argonne National Laboratory, Argonne, IL 60439

The fact that the emission spectrum of the microwave discharge in C₆₀/Ar mixtures is dominated by the Swan bands of C₂ has led us to propose that C₂ is the major species leading to the growth of diamond film. To see if this is a reasonable postulate, it will be necessary to determine the concentrations of C₂ in the plasma relative to other growth species such as CH₃• and C₂H₂. A study has been initiated to measure the concentration of these molecules by absorption spectroscopy. Thermodynamic calculations using reasonable assumptions of plasma temperature and pressure may also be a helpful guide to show trends of species concentrations as a function of hydrogen partial pressure. Qualitatively it would appear that low hydrogen partial pressures favor dehydrogenated species such as C₂H and C₂.

Recent calculations²¹ on tetrahedrally bonded, hydrogen-terminated carbon clusters up to C₄₆H₅₀ have been made to model the reaction of C₂ with the (110) surface of diamond. In a five-step reaction sequence, it has been found that two C₂ molecules can insert into the C-C bonds of the carbon cluster with low activation energies, and that each step in the sequence is exothermic. The overall energy release found theoretically is close to the experimentally known adsorption energy of C₂, 176 kcal/g mol C.

We have schematically modeled the reaction of C₂ with the reconstructed monohydrided diamond (100) surface and show a sequence of reaction steps in Fig. 12. The start of a new diamond lattice layer is shown in Fig. 13. The new layer is rotated 90° with respect to the original growth surface. The hydrogens terminating the original growth surface have migrated to the top of the new layer in accord with the theoretical predictions that this is energetically favorable.

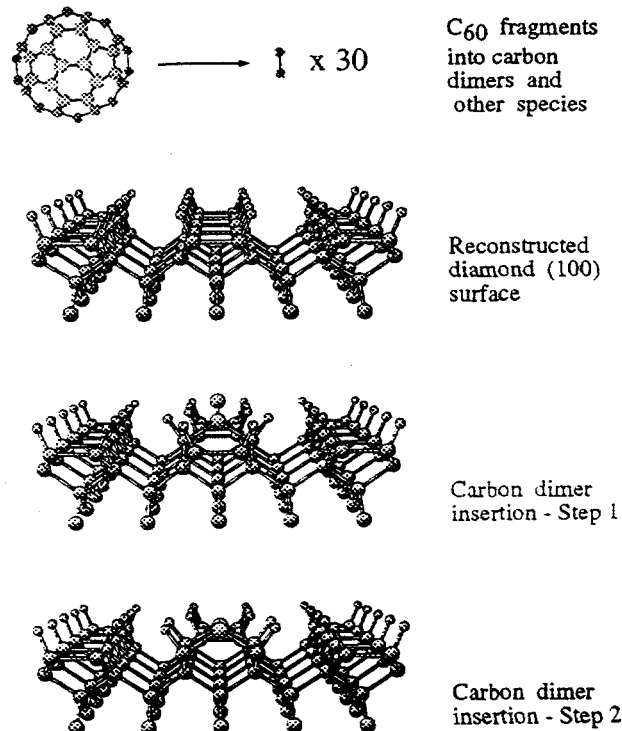


Fig. 12. Schematic diagram of C₂ insertion into the dimer rows of the diamond (100) surface.

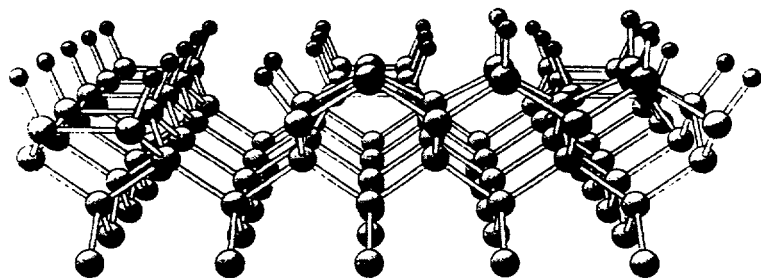


Fig. 13. Schematic diagram showing initial stages of growth of a new (100) diamond layer using C_2 as the growth species.

9. ACKNOWLEDGMENTS

Work supported by the U.S. Department of Energy, BES-Advanced Energy Projects, under Contract W-31-109-ENG-38.

10. REFERENCES

1. H. W. Kroto, J. R. Heath, S. C. O'Brien, R. E. Curl, and R. E. Smalley, *Nature* **318**, 162 (1985).
2. W. Krätschmer, L. D. Lamb, K. Fostiropoulos, and D. R. Huffman, *Nature* **347**, 354 (1990).
3. D. R. Kirklin, A. L. Smith, Y.-W. Hui, A. McGhie, W. J. Romanow, and G. Zimmerman, Abstract 690 FUL., 181st Mtg. Electrochemical Society, May 17-22, 1992, St. Louis, MO.
4. J. Abrefah, D. R. Olander, M. Balooch, and W. J. Siekhaus, *Appl. Phys. Lett.* **60**, 1313 (1992).
5. S. C. O'Brien, J. R. Heath, R. F. Curl, and R. E. Smalley, *J. Chem. Phys.* **88**, 220 (1988).
6. H.-G. Busmann, Th. Lil, and I. V. Hertel, *Chem. Phys. Lett.* **187**, 459 (1991).
7. J. F. Christian, Z. Wan, and S. L. Anderson, *J. Phys. Chem.* **96**, 3574 (1992).
8. D. M. Gruen, *Nucl. Inst. Methods in Physics Res. B* **78**, 118 (1993).
9. C. E. Klots, *Z. Phys. D* **21**, 335 (1992); *Chem. Phys. Lett.* **186**, 73 (1991); *J. Chem. Phys.* **90**, 4470 (1989); *Z. Phys. D* **20**, 105 (1991); *Acc. Chem. Res.* **21**, 16 (1988); *J. Phys. Chem.* **92**, 5864 (1988).
10. J. Drowart, R. P. Burns, G. DeMaria, and M. J. Inghram, *J. Chem. Phys.* **31**, 1131 (1959).
11. J. E. Butler and R. Woodin, *Phil. Trans. R. Soc. London A* **342**, 209 (1993).
12. F. G. Celii and J. E. Butler, *Ann. Rev. Phys. Chem.* **42**, 643 (1991).
13. D. N. Belton and S. J. Harris, *J. Chem. Phys.* **96**, 2371 (1992).
14. D. H. Horner, L. A. Curtiss, and D. M. Gruen, *Chem. Phys. Lett.* **233**, 243 (1995).
15. D. M. Gruen, S. Liu, A. R. Krauss, and X. Pan, *J. Appl. Phys.* **75**, 1758 (1994).
16. C. D. Zuiker, D. M. Gruen, and A. R. Krauss, *MRS Bulletin* **20**, 29 (1995); Proc. Electrochemical Society Symp. on Diamond Materials, Reno, NV, May 21-26, 1995 (in press).
17. H. Windischmann and G. F. Epps, *Diamond and Rel. Mat.* **1**, 656 (1992).
18. J. S. Luo, D. M. Gruen, A. R. Krauss, X. Z. Pan, and S. Z. Liu, Proc. Electrochemical Society Symp. on Fullerenes: Chemistry, Physics, and New Directions, Reno, NV, May 21-26, 1995 (in press).
19. B. K. Gupta, A. Malshe, B. Bushan, and V. V. Subramanian, *J. Tribology* **116**, 445 (1994).
20. P. K. Bachmann, H. J. Hagemann, H. Lade, D. Leers, D. U. Wiechert, H. Wilson, D. Fournier, and K. Plamann, *Diamond and Rel. Mat.* **4**, 820 (1995).
21. P. Redfern, D. A. Horner, L. A. Curtiss, and D. M. Gruen (manuscript in preparation).